Open-Ended Metallized Ceramic Coaxial Probe for High-Temperature Dielectric Properties Measurements

Shane Bringhurst, *Student Member, IEEE*, and Magdy F. Iskander, *Fellow, IEEE*

***Abstract*—A metallized ceramic coaxial probe has been developed for high temperature complex permittivity measurements. The probe is made of alumina and metallized with a 3.0-mil-thick layer of moly-manganese, and a 0.5-mil-thick protective coating of nickel plating. It is shown that based on carrying out the network analysis calibration procedure up to 1000°C, and on actual dielectric properties measurements, the probe provides accurate dielectric measurements over a broad frequency range (500 MHz to 3 GHz) and for temperatures up to 1000°C. An uncertainty analysis based on two different calibration techniques was also given to help quantify possible measurement errors.**

I. Introduction

OPEN-ENDED coaxial probes have been used for broadband dielectric properties measurements for several year [1]–[4]. The open-ended probe basically consists of a truncated section of a coaxial line, with an optional extension of a ground plane. The probe is connected to a vector network analyzer, HP8510B (45 MHz to 40 GHz), through a coaxial cable. The sample under test is placed flush with the probe and the values of the complex permittivity are then determined from the measurement of the input impedance of the probe. One of the critical elements in dielectric properties measurements, using an open-ended probe, is making a good contact between the probe and the material under test. It has been shown that air gaps on the order of fractions of a millimeter strongly influence the measured input impedance [5]. Several formulas are available for relating the measured input impedance to the complex permittivity of the material under test [6]–[7]. Even a commercial software package is available from Hewlett-Packard for making these measurements [8]. None of the available probes, however can be used at temperatures as high as 1000°C. This is due to problems with the differential thermal expansion of the inner and outer conductors in metal probes. Even the use of metals of small thermal expansion coefficients, such as kovar, has resulted in limited success and provided reasonable results for temperatures up to 800°C at which the thermal expansion coefficient of kovar increased significantly and hence affected the accuracy of the measurements [9]. Cavity perturbation techniques, on the other hand, although successfully applied for measurements at temperatures as high as 1400°C [10], are known to provide results over a narrow-band. In this paper we present the design, calibration and use of a metallized ceramic probe for high temperature dielectric properties measurements. In addition, the results of an uncertainty analysis will be presented to help quantify the errors associated with these measurements.

Manuscript received October 17, 1995; revised February 15, 1996.

The authors are with the Department of Electrical Engineering, University of Utah, Salt Lake City, UT 84112 USA

Publisher Item Identifier S 0018-9480(96)03797-0.

II. Probe Design and Impedance Characteristics

To solve the thermal expansion problem in coaxial probes we developed a metallized ceramic probe. However in designing any probe there are many important features to consider. Good impedance matching is important so as to minimize unnecessary reflections. Sufficiently large fringing fields are desired at the open end where the probe is placed in contact with the sample. This will help the field penetration in the sample under test and improve the accuracy of the characterization of the sample, and minimize contact errors between the probe and the sample under test. The probe dimensions need to be chosen carefully so that sufficient field penetration in the sample is provided at lower frequencies, and at the same time avoid radiation and multimodes at higher frequencies [11]. The metallization should also be of sufficient thickness so that skin depth problems are avoided at lower frequencies. The probe also needs to be of sufficient length, or a cooling system needs to be designed so as to minimize heating of the probe connectors. A brief description of the development of the probe design and preliminary results are discussed in other papers (conference proceedings) [12]–[13], while in this paper we will briefly mention the design, and present the results of more recent experimental results and the results from uncertainty analysis.

The probe was designed to be used in the frequency range of 500 MHz to 5 GHz. The probe was manufactured by WESGO Inc., by using an alumina rod and an alumina tube for both inner and outer conductors, of the coaxial probe, respectively. The dimensions of the rod and the tube were chosen so that the characteristic impedance of the probe would be 50 Ω. The tube and rod were metallized with about 3 mils of moly-manganese, and a 0.5-mil protective coating of nickel plating was then applied. To connect the probe to the standard accessories of a network analysis system, like the HP8510B, a GR–N-type connector was chosen, because of its broadband performance in the desired frequency range. The GR half of the connector was modified so that it could facilitate the connection of the open-ended coaxial probe.

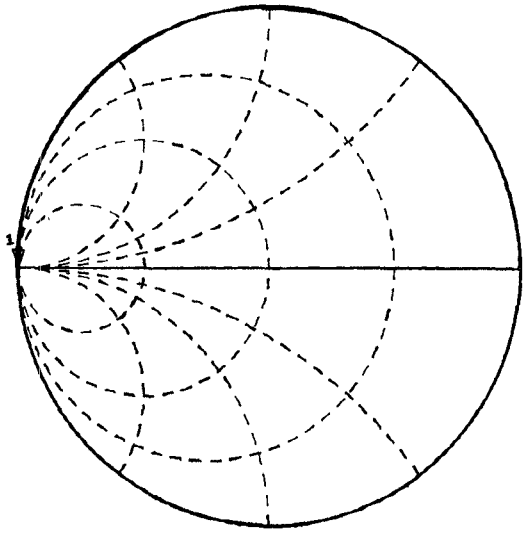

Fig. 1. Measured impedance of probe in the frequency range from 500 MHz to 3 GHz with calibration short attached.

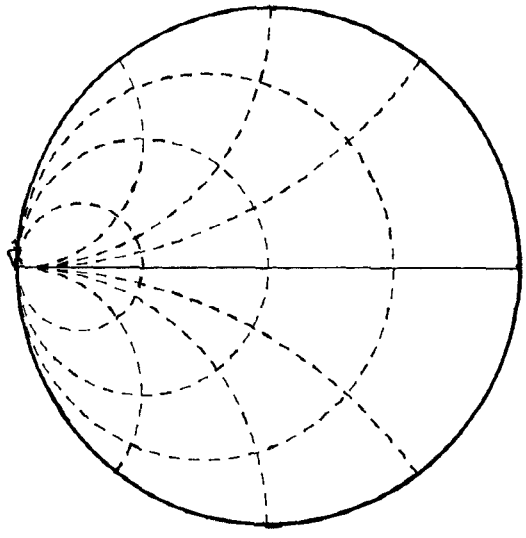

Fig. 2. Measured impedance of metallized probe, in the frequency range from 500 MHz to 3 GHz when a short was attached at 1000°C.

To verify that the thermal expansion of the metallized ceramic is minimal, the probe was calibrated with a short. Fig. 1 shows the measured impedance of the probe, in the frequency range from 500 MHz to 3 GHz, when the calibration short was attached. The probe and short were then heated up to 1000°C. Fig. 2 shows the measured impedance of the probe when terminated by a short at 1000°C. To emphasize the importance of developing a probe with very small thermal expansion coefficients, we constructed an identical probe of steel, and evaluated its calibration performance for temperatures up to 1000°C. Fig. 3 shows the obtained results from a short circuited metal probe at 1000°C. It is clear that having a coaxial probe with small thermal expansions coefficients, significantly improves the quality of the calibration procedure and certainly improves the accuracy of the dielectric measurement results. More discussion of measurement errors due to differential thermal expansion between the inner and outer conductors will be presented in the error analysis section of this paper.

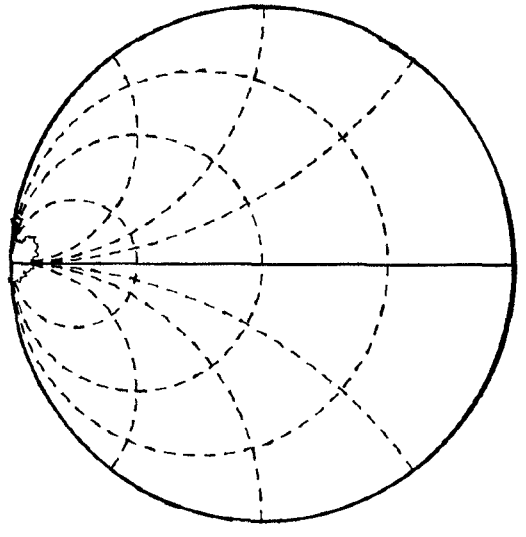

Fig. 3. Measured impedance of metal probe, in the frequency range from 500 MHz to 3 GHz when a short was attached at 1000°C.

III. High-Temperature Dielectric Measurements

A. Calibration Procedure

An important feature of the probe is the ability to carry out accurate and reproducible calibration procedures over a reasonably broad frequency band. Two different calibration procedures have been used with the metallized ceramic probe. One calibration procedure is the traditional 12-term error correction technique [14], and the other is a simpler derivative of the same procedure. Three known standards are required to determine the unknown coefficients in the 12-term error correction technique. An open, a short, and a standard material (usually deionized water), are the three commonly used calibration standards for low temperature open-ended probe measurements. For high-temperature measurements, however, another standard material must be used due to the low boiling point of water. Therefore we used an open, a short, and a standard ceramic material, for which ε^* is measured (using cavity perturbation techniques) for temperatures as high as 1000°C. These standards must be used at all temperatures, and this becomes very time consuming for measurements that are made up to 1000°C.

The simpler calibration technique is much easier to use and is not as time consuming, but in exchange the results are less accurate, as will be described later. For this calibration technique the probe is calibrated with the response calibration option which is available in automatic network analyzers such as the HP8753C. The response calibration is essentially used to remove the frequency response of the test setup. A response calibration only uses either a short or an open. The standard chosen depends upon the type of material being measured. We have found that if the dielectric properties of the material under test are closer to an open (e.g., ceramics like Al_2O_3, ZrO_2), then better results are obtained if the open standard is used.

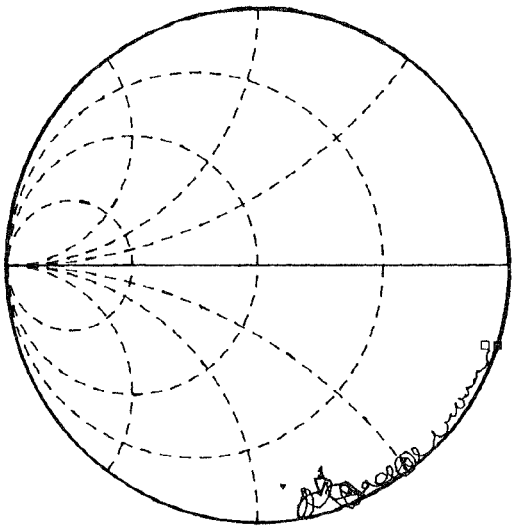

Fig. 4. Effect of response calibration with respect to open on measured admittance value. An Al_2O_3 sample was used in this experiment. ___ Admittance trace on network analyzer. ▽ Mark of the 3 GHz value. □ Mark of the 500 MHz value. ▼, ■ The 3 GHz and 500 MHz admittance values calculated, based on cavity perturbation measured complex permittivity values

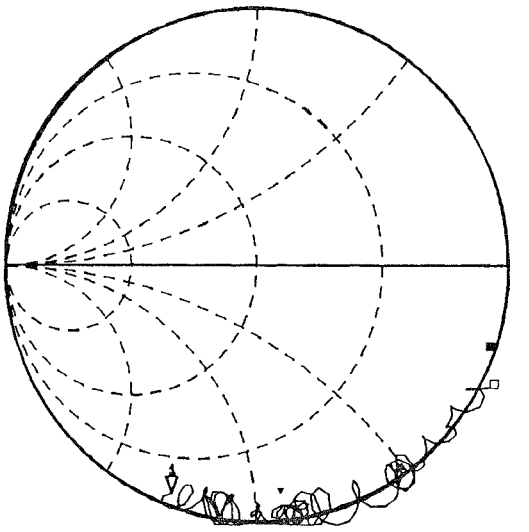

Fig. 5. Effect of response calibration with respect to short on measured admittance value. An Al_2O_3 sample was used in this experiment. ___ Admittance trace on network analyzer. ▽ Mark of the 3 GHz value. □ Mark of the 500 MHz value. ▼, ■ The 3 GHz and 500 MHz admittance values calculated, based on cavity perturbation measured complex permittivity values.

Likewise when the dielectric properties are closer to a short (e.g., water, methanol, and other materials of high dielectric properties), then better results are obtained if the short standard is used. Fig. 4 shows the measured admittance from 500 MHz to 3 GHz of Al_2O_3 after a response calibration with an open, and Fig. 5 shows the measured admittance from 500 MHz to 3 GHz of Al_2O_3 after a response calibration with a short. In Figs. 4 and 5 the admittance (Y) as measured by the probe is marked at 3 GHz with a ▽ mark and at 500 MHz with a □ mark. These two frequencies are the two extremes of the measured frequency range. These values of admittance are then compared with the admittance which corresponds to the complex permittivity values at these frequencies as determined using the cavity perturbation technique. The admittance from cavity measurements at 3 GHz is marked with a ▼ mark and the admittance at 500 MHz is marked with a ■ mark.

By comparing Figs. 4 and 5 it may be seen that the measured admittance after the calibration with an open provides more accurate results than the case when a short was used in the calibration. Fig. 6 shows the measured admittance from 500 MHz to 3 GHz of methanol after a response calibration with an open, and Fig. 7 shows the same measurement, but with a response calibration with a short. The values of admittance are compared with the admittance which corresponds to the complex permittivity values at these frequencies as determined using the Cole–Cole equation. In this case the measured admittance with a short calibration provides more accurate results (particularly at higher frequencies) as compared to calibration using an open circuit.

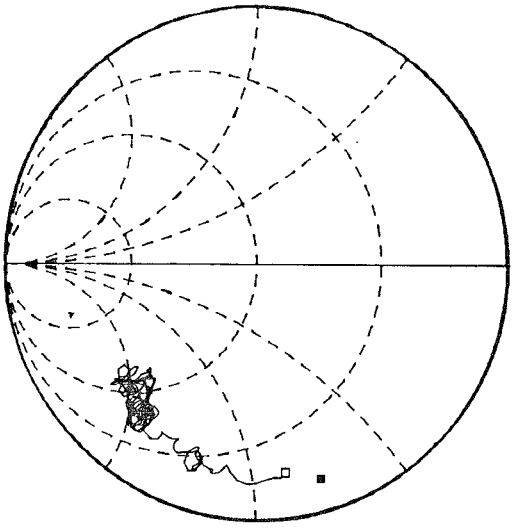

Fig. 6. Effect of response calibration with respect to open on measured admittance value A methanol sample was used in this experiment. ___ Admittance trace on network analyzer. ▽ Mark of the 3 GHz value. □ Mark of the 500 MHz value ▼, ■ The 3 GHz and 500 MHz admittance values calculated, based on cavity perturbation measured complex permittivity values.

B. Calculation Method

After calibration the standard material and the material under test are measured. As indicated earlier, to help improve the accuracy of the results, it is suggested that the standard material should be in the approximate dielectric range as that of the material under test. After measuring the admittance of both the material under test and the standard material, a correction factor C_{corr} is found using

$$C_{corr} = \frac{Y_{theor}}{Y_{meas}} \tag{1}$$

where Y_{meas} is the admittance that was measured with the probe. Y_{theor} is the theoretical admittance that is found by taking the theoretical values of the complex permittivity from literature and then calculating the admittance using the follow-

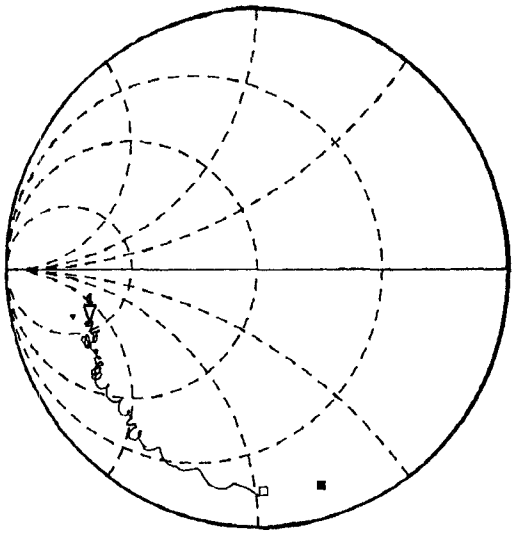

Fig. 7. Effect of response calibration with respect to short on measured admittance value. A methanol sample was used in this experiment. — Admittance trace on network analyzer. ▽ Mark of the 3 GHz value. □ Mark of the 500 MHz value. ▼, ■ The 3 GHz and 500 MHz admittance values calculated, based on cavity perturbation measured complex permittivity values.

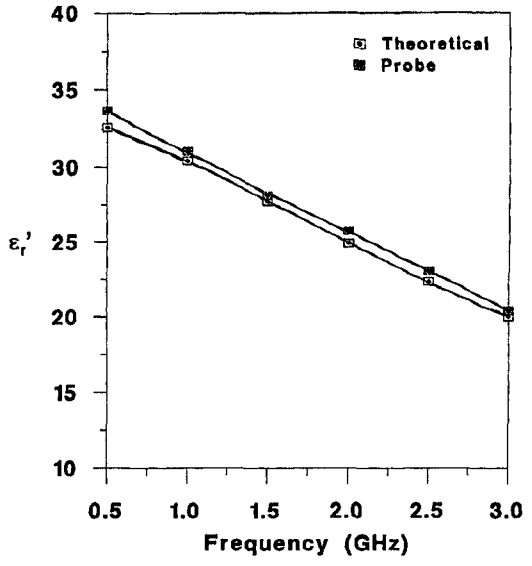

Fig. 8. ε_r' of methanol measured with metallized probe versus theoretical values in the frequency range from 500 MHz to 3 GHz.

ing integral equation derived by Levine and Papas [15]:

$$Y_{dut} = \frac{jk\varepsilon Y_o}{\ln\left(\frac{b}{a}\right)\sqrt{\varepsilon_i}} \times \int_0^\infty \frac{d\xi}{\xi(\xi^2 - k^2\varepsilon)^{5}} [J_o(\xi a) - J_o(\xi b)]^2 \quad (2)$$

where

ε_i dielectric constant of probe filler;
Y_o intrinsic admittance of the probe;
b radius of the outer conductor;
a radius of the inner conductor;
ε complex permittivity of sample;
Y_{dut} measured input admittance of the probe when brought in contact with sample under test;
$J_o(x)$ cylindrical Bessel function of argument x;
and where

$$k = \frac{2\pi}{\lambda_o}. \quad (3)$$

If the values for the standard material are not found in literature then the standard material is measured using cavity perturbation techniques (over limited frequency range) and those values are assumed to be the theoretical values. The corrected admittance of the material under test Y_{dutc} is then found by using

$$Y_{dutc} = C_{corr} Y_{dut} \quad (4)$$

where C_{corr} is the correction factor obtained using measurements on the standard material, and Y_{dut} is the measured admittance of the material under test. Once the corrected value of the admittance is found then the complex permittivity results (ε_r^*) can be obtained by substituting the values of Y_{dutc} into (2). For our purpose, we used a Mathcad® subroutine to carry out these calculations.

C. Measurement Results

Figs. 8 and 9 show the results of the complex permittivity of methanol measured at room temperature with the metallized ceramic open-ended probe. Fig. 8 shows the results of ε_r', and Fig. 9 shows the results of ε_r''. These results are compared with the theoretical complex permittivity values as given by the Cole–Cole equation

$$\varepsilon_r^* = \varepsilon_r' - j\varepsilon_r'' = \varepsilon_\infty + \frac{\varepsilon_s - \varepsilon_\infty}{1 + (j\omega\tau)^{1-a}} - j\frac{\sigma}{\omega\varepsilon_o} \quad (5)$$

where

σ ionic conductivity of the liquids;
τ relaxation time;
α distribution parameter;
ε_∞ optical relative permittivity;
ε_s static relative permittivity;
ω radian frequency.

The Cole–Cole parameters have been taken from the National Bureau of Standards data [15]. For the methanol measurements the calibration of the probe was done by taking a response calibration with respect to short and using deionized water as the standard material.

Figs. 10 and 11 show the obtained ε_r' results of ceramics that have been measured at room temperature with the metallized ceramic probe. For Fig. 10 the material under test was Al_2O_3 + 0.1 mol% MgO, and the standard material used for the measurements was ZrO_2 + 8 mol% Y_2O_3. For Fig. 11 the material under test was ZrO_2 + 8 mol% Y_2O_3, and the standard material was AlO_3 + 0.1 mol% MgO. The results in both cases are compared to the previously mentioned commercially available HP probe, and to cavity perturbation results [16]. When a line is fit to the data points it shows very good correlation between the three methods. However there are a few erroneous points in the metallized probe results. This is due to the more relaxed calibration method. It may be

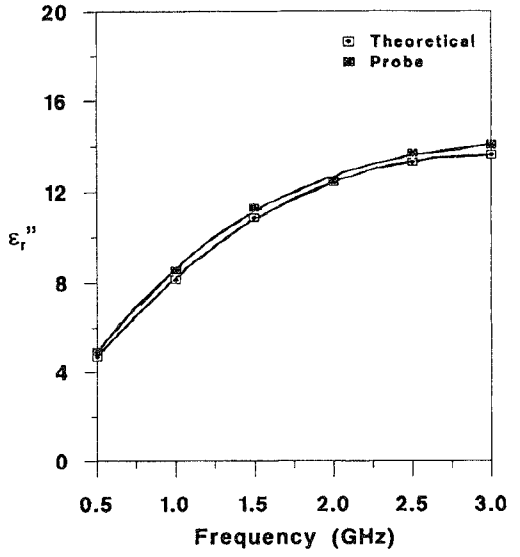

Fig 9. ε_r'' of methanol measured with metallized probe versus theoretical values for the frequency range from 500 MHz to 3 GHz.

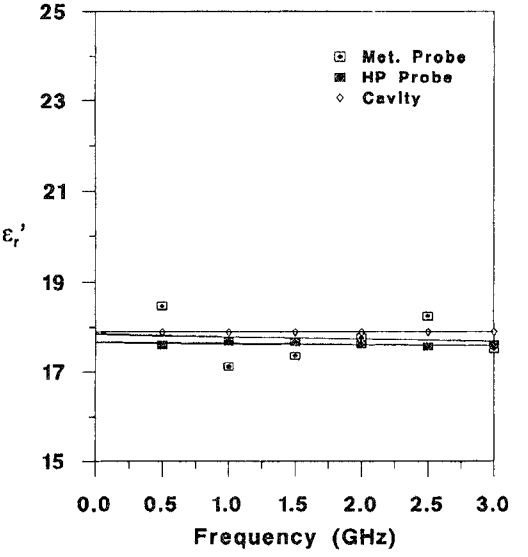

Fig. 11. ε_r' of $ZrO_2 + 8$ mol% Y_2O_3 measured after a response calibration versus cavity techniques and the commercially available Hewlett–Packard probe.

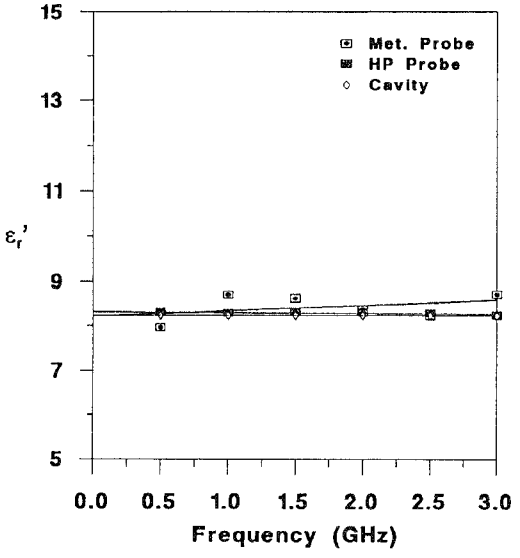

Fig. 10. ε_r'' of $Al_2O_3 + 0.1$ mol% MgO measured after a response calibration versus cavity techniques and the commercially available Hewlett–Packard probe.

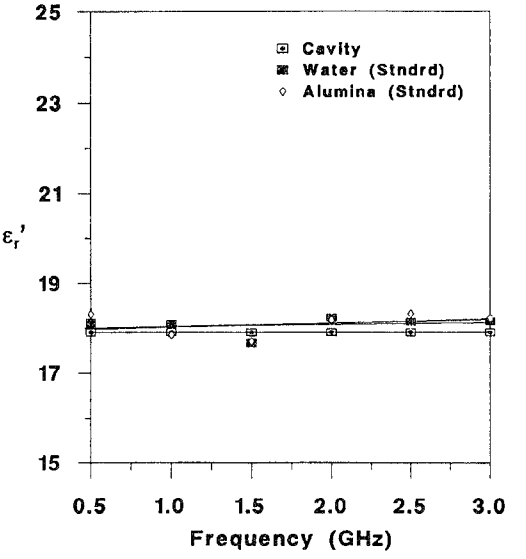

Fig. 12. ε_r' of $ZrO_2 + 8$ mol% Y_2O_3 measured after a full calibration using two different standard materials versus cavity techniques.

shown that in a calibration where only two standards are used that the results will not be as accurate as a method that uses the more complete calibration procedure.

Figs. 12 and 13 show the results of a more complete calibration on ZrO_2 + 8 mol% Y_2O_3. For these measurements the full 12-term error correction model was employed by using the three standards needed for the calibration. An open, a short, and then two different standard materials were used as the standard material so that a comparison could be made. Al_2O_3 + 0.1 mol% MgO was used as one of the standard materials and deionized water was used as the other. Fig. 12 shows the results for ε_r', and Fig. 13 shows the results for ε_r''.

In both figures a comparison is made between cavity perturbation techniques and measurements done on the same material, but just merely changing the standard material used in calibration. It is clear that these results are more accurate than the results shown in Fig. 11 because of the improved calibration procedure used in this case. It can also be pointed out that the standard material does not have to be in the general dielectric range of the material under test when a more complete calibration in performed.

After verification that the metallized probe worked well at room temperature the probe was used to make high-temperature measurements. Due to oxidation problems of the metallization at high temperatures, the probe must be used in a controlled atmosphere. Therefore a heating system has been developed that utilizes a molybdenum coil to heat the sample and the probe in a hydrogen atmosphere. The coil is typically

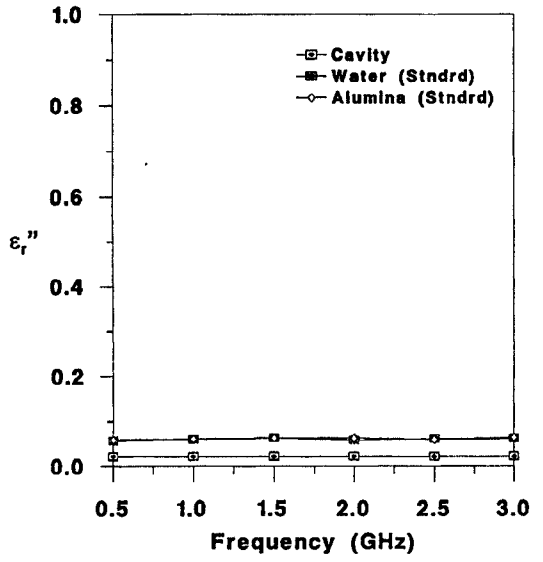

Fig. 13. ε_r'' of $ZrO_2 + 8$ mol% Y_2O_3 measured after a full calibration using two different standard materials versus cavity techniques.

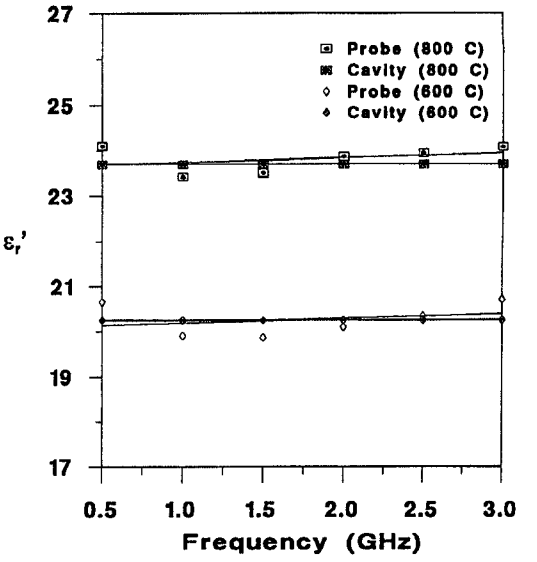

Fig. 15. ε_r' of $ZrO_2 + 8$ mol% Y_2O_3 versus cavity results at both 600 and 800°C in the frequency range from 500 MHz to 3 GHz.

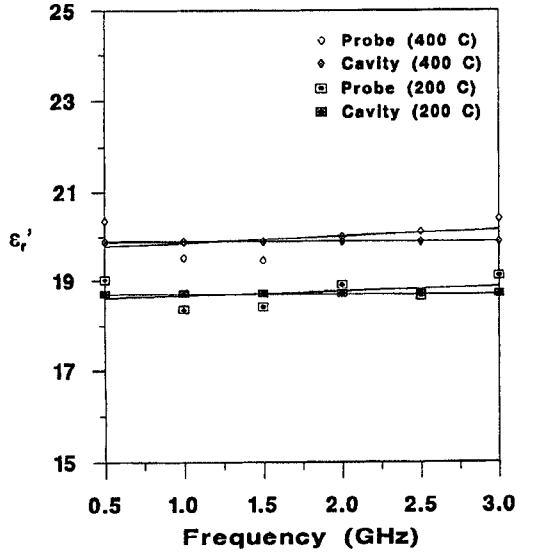

Fig. 14. ε_r' of $ZrO_2 + 8$ mol% Y_2O_3 versus cavity results at both 200 and 400°C in the frequency range from 500 MHz to 3 GHz.

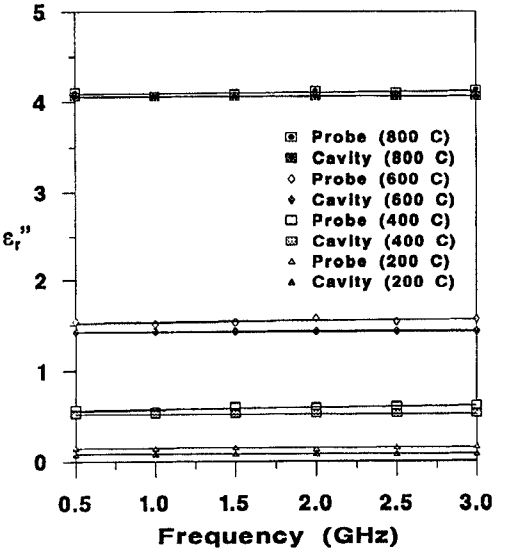

Fig. 16. ε_r'' of $ZrO_2 + 8$ mol% Y_2O_3 versus cavity results at 200, 400, 600, and 800°C in the frequency range of 500 MHz to 3 GHz.

4-in long, with a 2-in diameter. The coaxial probe is placed inside the coil with the coil centered at the interface between the probe and the sample. Figs. 14–16 show the results of ZrO_2 + 8 mol% Y_2O_3. For these measurements Al_2O_3 + 0.1 mol% MgO was used as the standard material. These measurements were done with the simpler response calibration. Fig. 14 shows the results of ε_r' compared to cavity perturbation results at 200 and 400°C. Fig. 15 shows the results of ε_r' compared to cavity perturbation results at 600 and 800°C. Fig. 16 shows the results of ε_r'' compared to cavity perturbation results at 200, 400, 600, and 800°C. A line has been fit to the data points in all three figures and it is clear that there is good agreement between the two measurements procedures. It is also clear that there are a few points that are not as accurate and, once again, this may be due to the simpler calibration method used. A full calibration would undoubtfully give more accurate overall results.

IV. Error Analysis

It has been mentioned earlier that a small air gap between the probe and the sample under test can cause significant errors in the measurements [5]. An analysis was therefore made to quantify the errors caused by the differential thermal expansion which is inherent in metal probes. In the heating up cycle the outer conductor will heat up faster than the inner conductor, and will therefore expand more than the inner conductor, thereby causing a measurement air gap between the inner conductor and the material under test. In the cooling down cycle the outer conductor will cool faster than the inner

TABLE I
COMPARISON BETWEEN THE FDTD REFLECTION COEFFICIENT RESULTS VERSUS ANALYTICAL DATA [5] FOR THE CASE OF AIR GAPS BETWEEN THE PROBE AND THE SAMPLE UNDER TEST PROBE DIMENSIONS ARE $a = 3.0$ MM, $b = 7.0$ MM, AND THE PROBE FILLER HAS $\varepsilon_r' = 2.54$, AND THE MATERIAL UNDER TEST HAS THE RELATIVE COMPLEX PERMITTIVITY $\varepsilon_r^* = 10.0 - j1.0$. RESULTS WERE CALCULATED AT $f = 1.0$ GHz

Probe liftoff from sample	Γ (Magnitude)		Γ (Phase in Degrees)	
	FDTD Model	Reference [5]	FDTD Model	Reference [5]
0.0 mm	0.950	0.952	-32.0	-29.0
0 5 mm	0 991	0 993	-10 8	-10 4
1 0 mm	0.998	0 996	-7 1	-7.0

TABLE II
COMPARISON OF MAGNITUDE AND PHASE OF INPUT IMPEDANCE WHEN AIR GAPS DUE TO DIFFERENTIAL THERMAL EXPANSIONS ARE PRESENT

% Difference with probe flush against material under test	Air gap between outer conductor and material under test			Air gap between inner conductor and material under test		
	0.25 mm	0 5 mm	1.0 mm	0.25 mm	0 5 mm	1 0 mm
Magnitude	34 4	73 0	104 7	296.6	480 0	985 7
Phase	4 4	5 4	13 8	5 5	6 1	12 1

TABLE III
COMPARISON OF COMPLEX PERMITTIVITY RESULTS WHEN CHARACTERISTIC IMPEDANCE VALUES ARE CHANGED DUE TO DIFFERENTIAL TRANSVERSE THERMAL EXPANSION BETWEEN THE INNER AND OUTER CONDUCTORS OF THE PROBE

% difference in	Change in characteristic impedance by			
	+5%	-5%	+10%	-10%
ε_r'	1 67%	2.48%	4.5%	2.76%
ε_r''	45%	123%	73 9%	157%

conductor, and will therefore shrink faster, thereby causing an air gap between the outer conductor and the material under test. Errors created by these air gaps were modeled using finite-difference time-domain (FDTD) simulations. The probe was first modeled flush against the material under test, and the input impedance was measured. Then an air gap, of 1.0, 0.5, and 0.25 mm, between the inner conductor and the material under test was modeled, and an air gap, of the same sizes, between the outer conductor and the material under test was also modeled. In all cases the input impedance was measured and compared to the original case. To check the accuracy of our FDTD model we first compared the FDTD results with those published earlier [5] for the case when the entire probe (both inner and outer conductors) were separated from the sample by an air gap. Table I shows comparison between the FDTD results and the analytical data published earlier [5] where it may be seen that there is a good agreement.

Table II gives the FDTD results of the error analysis for the high temperature case. Table II shows a comparison of both the magnitude and phase of the calculated input impedance when the probe is in contact with the sample versus when it is assumed that there is a differential thermal expansion between the inner and the outer conductors as described earlier.

It should be noted that the error analysis presented in this paper are different from those available in literature [5]. Unlike available analysis where uniform gaps between the probe and the sample are examined [5], the presented results show possible errors due to differential thermal expansions which are highly relevant to the topic of this paper. It may be desirable to report error analysis results for air gaps with dimensions smaller than 0.25 mm. This was however, very difficult using our presently available uniform mesh FDTD code. Memory requirements on the available work stations was simply prohibitive. It is possible to obtain such results using the variable mesh code presently under development [18] and these results will be reported in a future article.

Another analysis was also completed to examine the effect of thermal expansion on the characteristic impedance of the probe and hence its effect on the accuracy of the dielectric properties measurements. The ratio of the inner and outer conductors was changed by $\pm 5\%$ and $\pm 10\%$. $\pm 5\%$ change in the characteristic impedance corresponds to $\pm$ change in the radius of the outer conductor b or $\pm$ change in the radius of the inner conductor a. The new characteristic impedance (Z_o) of the probe was then calculated. The admittance (Y_o) can then be found, and substituted into (2) to find the new complex permittivity values. The new complex permittivity values were then compared to the original values obtained for a probe with an characteristic impedance of 50 Ω. Table III gives the results of the comparisons.

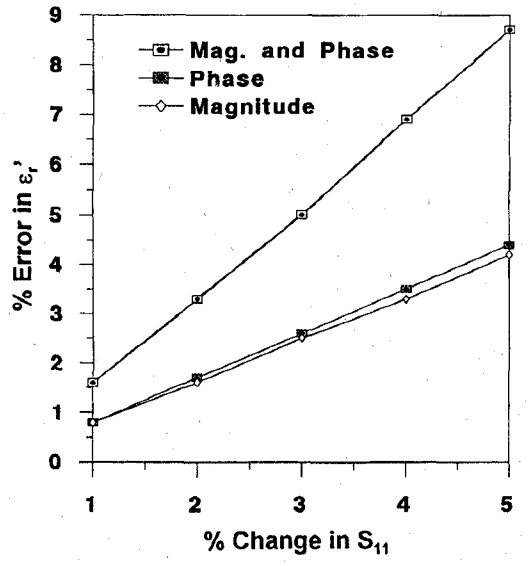

Fig. 17. Error analysis of ε_r' by changing S_{11} of the material under test.

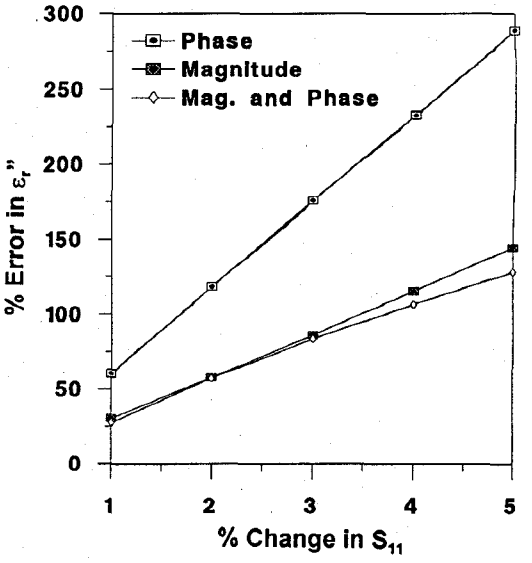

Fig. 18. Error analysis of ε_r'' by changing S_{11} of the material under test.

From the results in Tables II and III it may be noted that longitudinal and transverse differential thermal expansion of the probe may have significant effect on the dielectric properties measurements. The development of the metallized ceramic probe, therefore, is highly important and certainly needed.

Finally an analysis was made to estimate how the errors in the measurement of S_{11} (since the S_{11} term is what is measured) could affect the complex permittivity results. An actual measurement was made and then S_{11} was intentionally varied to see how the results for the complex permittivity would change. The magnitude and phase of S_{11} were changed from 1–5% (both separately and then together) and then substituted back into the 12-term error correction model to obtain a new Y_{dut}. The value of the complex permittivity is then obtained by using (2). Figs. 17 and 18 show the absolute value of the resulting errors in the value of the complex permittivity by measurement errors in S_{11} when the probe was in contact with the material under test.

Similar analysis was done by altering S_{11} from 1–5% (both magnitude and phase separately and then together) when calibration was made on the standard material. Figs. 19 and 20 show the errors in ε_r' and ε_r'' of the material under test as a result of errors in S_{11} when the probe was in contact with the standard material.

By examining Figs. 17–20 it can be seen that for only a 5% error in the measurement of S_{11}, of the material under test, the error can be as high as 8.7% for ε_r', and as high as 289.1% for ε_r''. It can also be seen that for only a 5% error in the measurement of S_{11}, of the standard material, the error can be as high as 7.1% for ε_r', and as high as 261.5% for ε_r''. This leads to the conclusion that for accurate dielectric measurements using the open-ended coaxial probe, errors in S_{11} for standard materials, and for the material under test should be less than 1%. Other errors that may be introduced from differential thermal expansions are expected to further reduce the accuracy of the results.

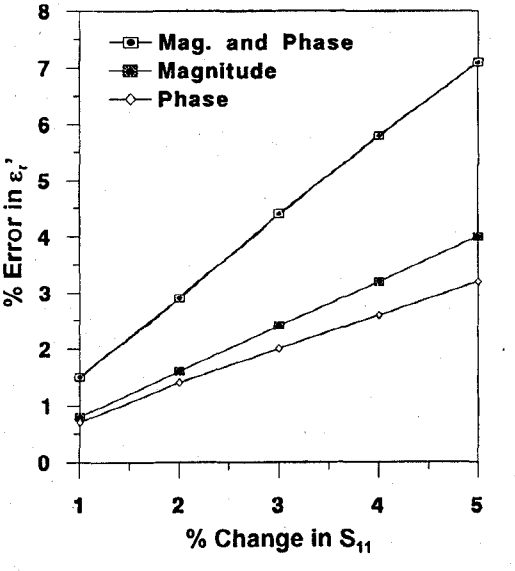

Fig. 19. Error analysis of ε_r' by changing S_{11} of the standard material.

It is shown that the use of the metallized ceramic probe will significantly enhance the accuracy and capability of this dielectric properties measurement system.

V. Summary and Conclusion

An open-ended metallized ceramic coaxial probe has been developed to provide accurate dielectric properties results over a broad frequency band and up to 1000°C. The probe was made of alumina and metallized with 3-mil thickness of moly-manganese and a 0.5-mil protective coating of nickel. This metallized ceramic probe ensures more accuracy than any type of metal probe because of the minimal thermal expansion difference between the inner and outer conductors. Typical frequency range of the developed probe is from 500 MHz to 5 GHz. At lower frequencies, a larger coaxial probe is expected to provide improved accuracy, while a coaxial probe with

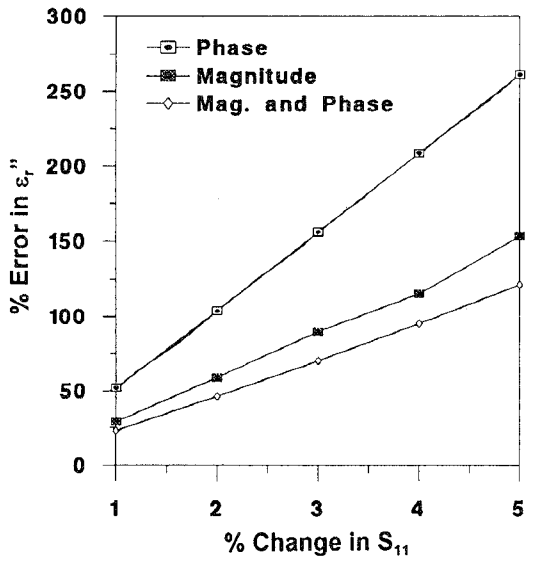

Fig. 20. Error analysis of ε_r'' by changing S_{11} of the standard material.

smaller inner and outer conductor dimensions, are expected to help improve the accuracy of these measurements at higher frequencies.

Two different calibration methods have been employed in the presented measurement results. One method consists of a response calibration with either a short-circuit or an open-circuit, and a standard material, which should have similar complex permittivity values as the material under test. The other calibration method is the three calibration standard method used to determine the unknown coefficients in the 12-term error correction model in the vector network analyzer. There is a trade-off in deciding which calibration to use. The former method is much simpler and less time consuming than the later, but the results are not as accurate. In the later method any standard material can be used as the calibration standard as long as the dielectric properties are well known.

An error analysis has been given to show that relatively small errors in the measurement of S_{11} of either the material under test or the standard material can result in significant errors in the complex permittivity results. The resulting errors are much greater in ε_r'' than in the ε_r' values. This is due to open-ended coaxial probes inherent problem of not being suitable for measuring the loss factor accurately in particularly low-loss materials. The broadband capabilities of this probe, however, and the simplicity of use continues to make this measurement technique an attractive and frequently used one. An error analysis has also been given to show that the differential thermal expansion which is inherent in metal probes can lead to erroneous results in the measurement of the complex permittivity. This can be due to both air gaps between the probe and the material under test, and changes in the characteristic impedance of the inner and outer conductors of the probe.

REFERENCES

[1] E. C. Burdette, F. L. Cain, and J. Seals, "*In vivo* probe measurement technique for determining dielectric properties at VHF through microwave frequencies," *IEEE Trans. Micro. Theory Tech.*, vol. MTT-28, pp. 414–427, 1980.

[2] E. Tanabe and W. T. Joines, "A nondestructive method for measuring the complex permittivity of dielectric materials at microwave frequencies using an open transmission line resonator," *IEEE Trans. Instrum. Meas.*, vol. IM-25, pp. 222–226, 1976.

[3] D. Misra *et al.*, "Noninvasive electrical characterization of materials at microwave frequencies using an open-ended coaxial line: Test of an improved calibration technique," *IEEE Trans. Micro. Theory Tech.*, vol. 38, pp. 8–14, 1990.

[4] O. M. Andrade, M. F. Iskander, and S. Bringhurst, "High temperature broadband dielectric properties measurement techniques," *Microwave Processing of Materials III*, vol. MRS-269, pp. 527–539, 1992.

[5] J. Baker-Jarvis, M. D. Janezic, P. D. Domich, and R. G. Geyer, "Analysis of an open-ended coaxial probe with lift-off for nondestructive testing," *IEEE Trans. Instrum. Meas.*, vol. 43, pp. 711–718, 1994. (Errata for the dimensions of the probe listed in the captions of Figs. 4 and 5 as well as for mislabeling Figs. 10 and 11 will be published by the authors of [5] soon).

[6] P. De Langhe, K. Blomme, L. Martens, and D. De Zutter, "Measurement of low-permittivity materials based on a spectral-domain analysis for the open-ended coaxial probe," *IEEE Trans. Instrum. Meas.*, vol. 42, pp. 879–886, 1993.

[7] C. Li and K. Chen, "Determination of electromagnetic properties of materials using flanged open-ended coaxial probe-full-wave analysis," *IEEE Trans. Instrum. Meas.*, vol. IM-44, pp. 19–27, 1995.

[8] D. Blackham, "Calibration method for open-ended coaxial probe/vector network analyzer system," *Microwave Processing of Materials III*, vol. MRS-269, pp. 595–599, 1992.

[9] M. F. Iskander, and J. B. Dubow, "Time-and frequency-domain techniques for measuring the dielectric properties of rocks: A review," *J. Microw. Power*, vol. 18, no. 1, pp. 55–74, 1983.

[10] R. M. Hutcheon *et al.*, "RF and microwave dielectric measurements to 1400°C and dielectric loss mechanisms," *Microwave Processing of Materials III*, vol. MRS-269, pp. 541–551, 1992.

[11] S. Bringhurst, "Metallized ceramic open-ended coaxial probe for broadband high temperature dielectric properties measurements," M.S. thesis, Univ. Utah, Salt Lake City, UT, Mar. 1995.

[12] S. Bringhurst, M. F. Iskander, and O. A. Andrade, "New metallized ceramic coaxial probe for high-temperature dielectric properties measurements," *Microwaves: Theory and Application in Materials Processing II, Ceramic Trans.*, vol. 36, pp. 503–510, 1993.

[13] S. Bringhurst, M. F. Iskander, and P. Gartside, "FDTD simulation of an open-ended metallized ceramic probe for broadband high-temperature dielectric properties measurements," *Microwave Processing of Materials IV*, vol. MRS-347, pp. 221–228, 1994.

[14] J. Fitzpatrick, "Error models for systems measurements," *Microwave J.*, vol. 21, no. 5, pp. 63–66, 1978.

[15] H. Levine and C. H. Papas, "Theory of the circular diffraction antenna," *J. Appl. Phys.*, vol. 22, no. 1, 1951.

[16] *Tables of Dielectric Dispersion Data for Pure Liquids and Dilute Solutions*, National Bureau of Standards Circular 589, Nov. 1, 1958.

[17] S. Bringhurst, M. F. Iskander, and O. M. Andrade, "High-temperature dielectric properties measurements of ceramics," *Microwave Processing of Materials III*, vol. MRS-269, pp. 561–568, 1992.

[18] Z. Huang, J. Tucker, and M. F. Iskander, "FDTD modeling of realistic microwave sintering experiments," in *IEEE AP-S Symp. Dig.*, vol. 3, pp. 1798–1801, 1994.

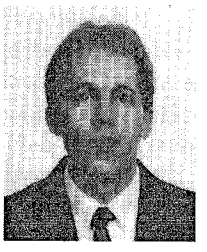

Shane Bringhurst (S'95) received the B.S. and M.S. degrees in electrical engineering from the University of Utah, Salt Lake City, UT, in 1992 and 1995, respectively. He is currently working on a Ph.D. degree at the University of Utah in the area of electromagnetics and microwaves.

He is both a Research and Teaching Assistant. His research includes: dielectric properties measurements, microwave sintering of ceramics, microwave and RF drying of ceramics, and numerical techniques in electromagnetics.

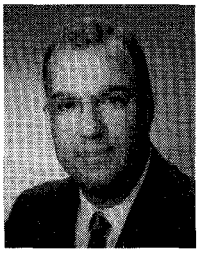

Magdy F. Iskander (F'93) received the B.Sc (Hon.) degree from the University of Alexandria in 1969, and M.Sc. and Ph.D. degrees from the University of Manitoba, Winnipeg, Man., Canada, in 1972 and 1975, respectively.

He is Professor of Electrical Engineering at the University of Utah, Salt Lake City. He is also the Director of the NSF/IEEE Center for Computer Applications in Engineering Education (CAEME) and Director of the State Center of Excellence for Multimedia Education and Technology. In 1986, he established the Engineering Clinic Program to attract industrial support for projects to be performed by engineering students at the University of Utah. Since then, more than 60 projects have been sponsored by 21 corporations from across the United States. He is also the Director of the *C*onceptual *L*earning *o*f *S*cience (COLOS) USA Consortium which is sponsored by Hewlett-Packard Company and has eleven Member universities from across the United States. He edited a book on *Microwave Processing of Materials* (Materials Research Society, 1994), and authored a textbook on *Electromagnetic Fields and Waves,* (Englewood Cliffs, NJ: Prentice-Hall, 1992). He edited the *CAEME Software Book,* vol. I, 1991; Vol. II, 1994; and co-edited two other books on *Microwave Processing of Materials,* (Materials Research Society, 1991 and 1992). He edited two special issues of the *Journal of Microwave Power,* one on "Electromagnetics and Energy Applications," March 1983, and the other on "Electromagnetic Techniques in Medical Diagnosis and Imaging," September 1983. He also edited a special issue of the *ACES Journal* on computer-aided electromagnetics education and the *Proceedings of the 1995 International Conference on Simulation in Engineering Education.* He is the editor of the journal *Computer Applications in Engineering Education (CAE),* (New York: Wiley). He has published more than 150 papers in technical journals and made numerous presentations in technical conferences. His present fields of interest include the use of numerical techniques in electromagnetics.

Dr. Iskander has received the Curtis W. McGraw ASEE National Research Award for outstanding early achievements, the ASEE George Westinghouse National Award for innovation in Engineering Education, and the 1992 Richard R. Stoddard Award from the IEEE EMC Society. He is a Distinguished Lecturer for the Antennas and Propagation Society of IEEE. He is a member of the National Research Council Committee on Microwave Processing of Materials.